Purification of the Small Mechanosensitive Channel of *Escherichia coli* (MscS): the Subunit Structure, Conduction, and Gating Characteristics in Liposomes

Sergei Sukharev
Department of Biology, University of Maryland, College Park, Maryland 20742 USA

ABSTRACT The small mechanosensitive channel, MscS, is a part of the turgor-driven solute efflux system that protects bacteria from lysis in the event of osmotic downshift. It has been identified in *Escherichia coli* as a product of the orphan *yggB* gene, now called *mscS* (Levina et al., 1999, *EMBO J.* 18:1730). Here I show that that the isolated 31-kDa MscS protein is sufficient to form a functional mechanosensitive channel gated directly by tension in the lipid bilayer. MscS-6His complexes purified in the presence of octylglucoside and lipids migrate in a high-resolution gel-filtration column as particles of ~200 kDa. Consistent with that, the protein cross-linking patterns predict a hexamer. The channel reconstituted in soybean asolectin liposomes was activated by pressures of 20–60 mm Hg and displayed the same asymmetric I-V curve and slight anionic preference as in situ. At the same time, the single-channel conductance is proportional to the buffer conductivity in a wide range of salt concentrations. The rate of channel activation in response to increasing pressure gradient across the patch was slower than the rate of closure in response to decreasing steps of pressure gradient. Therefore, the open probability curves were recorded with descending series of pressures. Determination of the curvature of patches by video imaging permitted measurements of the channel activity as a function of membrane tension (γ). $Po(\gamma)$ curves had the midpoint at 5.5 $\pm$ 0.1 dyne/cm and gave estimates for the energy of opening $\Delta G = 11.4 \pm 0.5\,kT$, and the transition-related area change $\Delta A = 8.4 \pm 0.4$ nm^2 when fitted with a two-state Boltzmann model. The correspondence between channel properties in the native and reconstituted systems is discussed.

INTRODUCTION

Perception of mechanical force by living organisms takes on many different forms. Hearing and proprioception in animals or gravitropic responses in plants involve elaborate multicomponent mechanisms (Gillespie and Walker, 2001; Chen and Masson, 1999). In prokaryotes, mechanosensation is apparently limited to the detection of osmotic forces manifested as intracellular turgor pressure. Turgor pressure is considered an important parameter for the processes of cell wall expansion and bacterial cell division (Koch, 1997) and presumed to be tightly regulated. Under strongly hypotonic conditions, when the elastic cell wall is stretched beyond certain limits, internal pressure translates into membrane tension, which can produce cell lysis (Levina et al., 1999).

Bacteria survive and grow in a wide range of external osmolarities because of powerful adaptation mechanisms (Csonka and Hanson, 1991;Wood, 1999). Shifts to a higher osmolarity trigger an uptake, exchange, or synthesis of internal osmolytes de novo, controlled by several types of inner membrane receptors (Wood, 1999). However, to escape excessive turgor pressure and a menace of lysis under hypotonic conditions, bacteria instantly release internal osmolytes via large nonselective stretch-activated channels (Booth and Louis, 1999). The latter probably represent the simplest and most ancient example of a membrane-based mechanosensory response. First reported by Martinac et al. (1987), these bacterial channels became convenient models for detailed biophysical studies of primary mechanosensory mechanisms (Spencer et al., 1999; Blount et al., 1999).

Patch-clamp survey of giant spheroplasts and reconstituted membrane preparations revealed at least two types of mechanosensitive (MS) channels in *Escherichia coli* (Sukharev et al., 1993; Berrier et al., 1996). The smaller channel, MscS, has slight anionic preference, conducts at 0.9–1 nS under typical patch-clamp conditions, and activates at moderate pipette pressures (50–100 mm Hg). The large channel, MscL, conducts nonselectively at ~3 nS, and requires 1.5–1.7 times higher pressure for its activation as compared with MscS. Both channels survive solubilization with a mild detergent and remain functional when reconstituted in liposomes (Sukharev et al., 1993).

Historically, the larger channel, MscL, was isolated, cloned, and underwent structural characterization first (Sukharev et al., 1994; Chang et al., 1998). Although the activities of MscS were described earlier (Martinac et al., 1987), it took longer to identify the small channel as a molecular entity. Using extensive sequence analysis of homologs of the potassium efflux protein KefA in the *E. coli* genomic database, knock-outs, and patch-clamp analysis, Levina et al. (1999) determined that the population of small MS channels in *E. coli* consists of at least two species, one of which requires the product of *kefA* itself and the other which relies on the presence of *yggB* (*mscS*). The functional product of *mscS* gene is apparently more abundant than that of *kefA* and exhibited a pronounced time-dependent adap-

Submitted January 10, 2002, and accepted for publication March 20, 2002.
Address reprint requests to Sergei Sukharev, Department of Biology, University of Maryland, College Park, MD 20742. Tel.: 301-405-6923; Fax: 301-314-9358; E-mail: ss311@umail.umd.edu.

0006-3495/02/07/290/09 $2.00

tation upon activation by pressure. MscS exhibits a high degree of organizational similarity but limited sequence similarity (20%) to the C-terminal 224 amino acid fragment of KefA (Levina et al., 1999; McLaggan et al., 2002; S. Miller and I. R. Booth, personal communication). MscS has multiple homologs in *E. coli* itself and in other bacteria, but exhibits no significant similarity to any other well characterized group of ion channels.

In the present work, I address the question of whether the MscS protein alone is capable of forming functional MS channels. The molecular size of the tag-purified MscS has been determined and the subunit structure of the complex assessed by covalent cross-linking. The purified protein was subsequently reconstituted in liposomes and found to form functional channels with conductive properties similar to those in spheroplasts. By measuring MscS activities with simultaneous imaging of large liposome patches, the open probability as a function of membrane tension was determined, and the spatial and energetic parameters for the opening transition extracted.

MATERIALS AND METHODS

Genetic manipulations

The sequence of the fragment of *E. coli* chromosome containing *yggB* (66.11′ min) was obtained from the EcoGene database (accession #EG11160). The 860 bp ORF plus 40 bp upstream sequence was polymerase chain reaction (PCR)-amplified from the AW405 strain (a subclone of *E. coli* K12, provided by J. Adler, University of Wisconsin) and first cloned into the pGEM-T vector (Promega, Madison, WI). The 3′ end of the ORF was subsequently extended with six His codons using two PCR steps and cloned as a BglII-*Xho*I fragment into the pB10b vector (Blount et al., 1996) behind the inducible P_{UVlac} promotor. Sequencing has identified a single base change compared with the sequence originally deposited in the database, which resulted in the Val280 to Met substitution. This conservative substitution was confirmed in several PCR products independently amplified from our AW405 stock and apparently represents a natural variant of the gene rather than a PCR error.

Protein isolation

MscS-6His was expressed in MJF455 *mscL-*, *mscS-E. coli* cells (Levina et al., 1999) kindly provided by I. R. Booth (University of Aberdeen, UK). Four liters of culture were grown in standard Luria-Bertani (LB) medium, induced with 0.7 mM IPTG for 1 h, and harvested at OD_{600} of 1.2. The cells were washed once with a 50 mM KP_i buffer containing 5 mM $MgCl_2$ and French-pressed at 16,000 psi in the presence of 1 mM phenylmethylsulfonyl fluoride (PMSF). The homogenate was treated with DNAse (0.05 mg/ml) and lysozyme (0.2 mg/ml) for 15 min. Membranes were then collected by a 25-min ultracentrifugation at 30,000 rpm in an SW40Ti (Beckman, Palo Alto, CA) rotor and stored frozen at −80°C.

Extraction and purification procedures were carried out at room temperature. Defrosted membrane pellets of ~0.8 g wet weight were solubilized in 20 ml of low-imidazole buffer (100 mM NaCl, 10 mM imidazole, pH 7.2), containing 3% octylglucoside (OG, Calbiochem, La Jolla, CA) and 1 mM PMSF, using a loose piston glass homogenizer. The extract was cleared from insoluble particles by a 15-min centrifugation at 20,000 *g*. Four milliliters of Ni-NTA agarose (Qiagen, Valencia, CA) was added to the supernatant and the suspension was gently rotated for 15 min to achieve complete batch-loading of the resin. The agarose was then packed by gravity in a 15-ml glass column (Kontes Glassware, Vineland, NJ) and washed with 30 ml of low-imidazole buffer supplemented with 1% OG and 0.02% phospholipid (asolectin, Soybean Lecithin type II, Sigma, St. Louis, MO). The column was then attached to a fast protein liquid chromatography (FPLC) system (Pharmacia, Uppsala, Sweden) via a flow adapter and additionally washed with 20 ml of the low-imidazole buffer at 1 ml/min. Bound proteins were then eluted with a linear 10 to 500 mM imidazole gradient (30 min, 1 ml/min), followed by a sustained 10-min wash by a high-imidazole buffer (100 NaCl, 0.5 M imidazole, 1% OG and 0.02% phospholipid). The entire eluate was typically distributed among 11 fractions of 4 ml. In preliminary experiments the protein composition of each individual fraction was determined with sodium dodecyl sulfate-polyacrylamide gel electrophoresis (SDS-PAGE), and the pure MscS band was found in the second half of the gradient (fractions 5–11). MscS-containing fractions were pooled together and concentrated to 3 ml with a Centriprep 30 concentrator (Millipore, Bedford, MA). The protein was then transferred into a phosphate (P) buffer (100 mM NaCl, 30 mM NaPi, pH 7.2, 1% OG, 0.02% phospholipid) using a desalting column (PD-10, Pharmacia) and finally assayed using a bicinchoninic acid (BCA) protein assay kit (Pierce, Rockford, IL).

Biochemical characterization of MscS complexes

Sizing chromatography was performed on a Superose 6 FPLC column (Pharmacia), precalibrated with size-exclusion standards (Bio-Rad, Hercules, CA) in the P buffer in the absence of detergent and lipid at a 0.3 ml/min flow rate. The column was then reequilibrated with the P buffer containing OG and lipid, and the purified MscS was chromatographed at the same flow rate. The position of the MscS peak was detected by UV absorbance and confirmed by SDS-PAGE of individual 0.5-ml fractions.

The subunit structure of MscS complexes was assessed by covalent cross-linking with the 11-Å spacer arm bifunctional reagent disuccinymidilsuberate (DSS, Pierce). Five equal aliquots of purified MscS (each containing ~0.2 mg of protein), were diluted with the OG/lipid-containing P buffer to 4 ml and gently rotated with various concentrations of DSS (0–1 mM) for 15 min in 5-ml screw-cap tubes. The reactions were quenched by adding Tris buffer (to 150 mM, pH 8.0), and rotating for additional 5 min. The contents of each tube was then concentrated with a Centricon 30 (Millipore) to a final volume of ~100 μl, mixed with 30 μl of 2× Laemmli sample buffer, heated up at 60°C for 5 min, and resolved with SDS-PAGE. The protein bands were visualized by Coomassie or silver staining.

Channel reconstitution into liposomes, electrical recording, and imaging

Purified MscS-6His was mixed with 5 mg of OG-dissolved asolectin at a protein-to-lipid ratio of ~1:200 (w/w). The mixture (~1 ml) was dialyzed for 24 h against 2 l of buffer (50 mM NaCl, 5 mM Tris-HCl, pH 7.2) with three changes in the presence of Calbiosorb detergent-adsorbing beads (Calbiochem). The proteoliposomes were pelleted in an Airfuge (Beckman, Fullerton, CA), resuspended in 30 μl of 10 mM MOPS buffer with 10% ethylene glycol, and subjected to a dehydration-rehydration cycle on coverslips as previously described (Delcour et al., 1989; Sukharev et al., 1993). Small amounts of rehydrated lipid material were transferred to a patch chamber filled with the recording buffer (200 mM KCl, 40 mM MgCl2, 10 mM HEPES, pH 7.2) where they formed transparent "blisters." The blisters, visible under phase contrast, were subjected to patch-clamp examination. Currents were recorded with borosilicate glass pipettes (Drummond, Broomall, PA) using an Axopatch 200B amplifier and Pclamp 6 software (Axon Instruments, Union City, CA) for data acquisition. Pressure

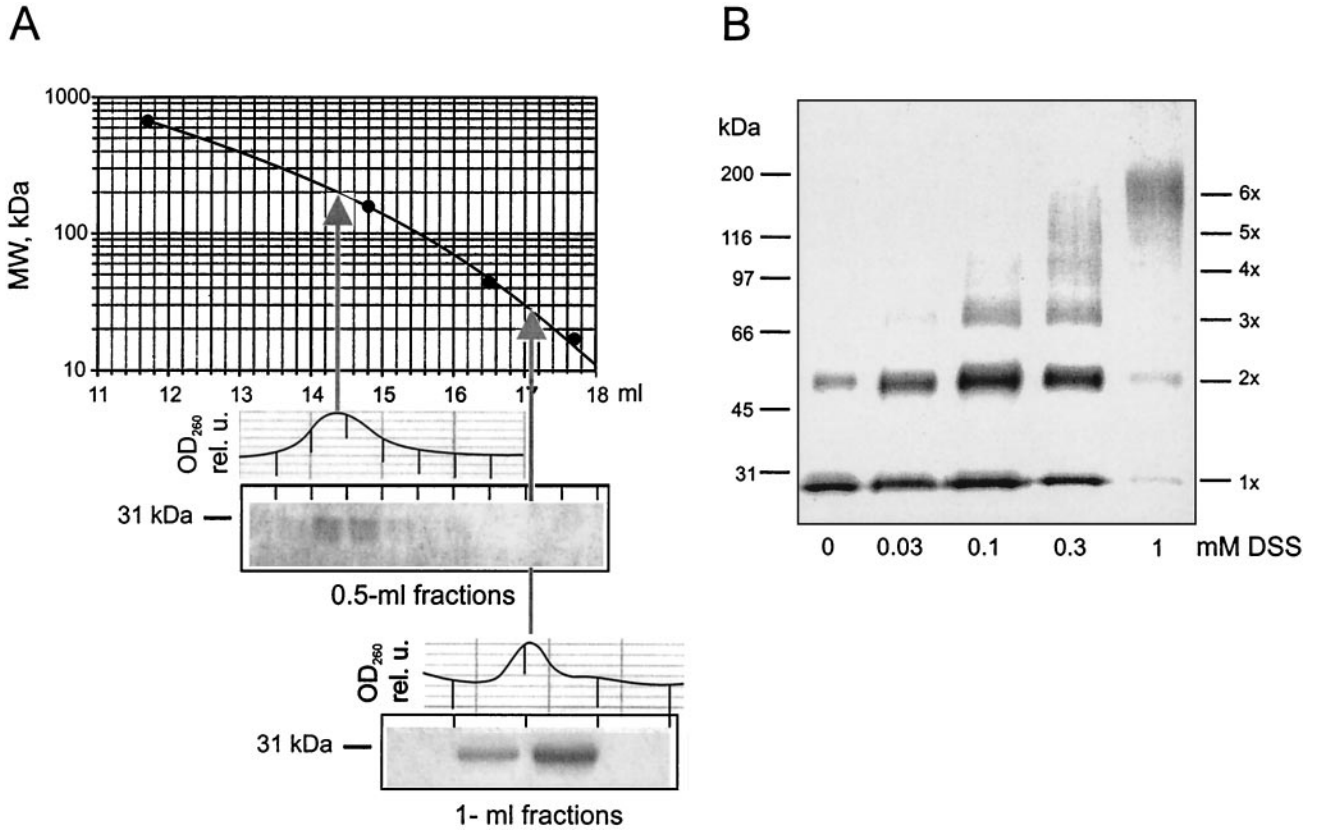

FIGURE 1 The assessment of the subunit structure of MscS-6His. (*A*) Results of size-exclusion chromatography on a Superose 6 FPLC column. The chromatogram and gel obtained in the presence of detergent lipid (*middle*) indicate that MscS-6His emerges as a peak in two 0.5-ml fractions near the 200-kDa mark on the calibration curve (*top*). In the absence of lipid (detergent only) MscS elutes as a peak of ~30 kDa (*bottom*). (*B*) Cross-linking of MscL-6His with DSS. The products obtained with varied DSS concentrations were resolved in 4–15% SDS-PAGE stained with Coomassie blue. A small amount of subunit dimers was typically present in the control. The highest band in the ladder of products represents a cross-link of six 31-kDa subunits, suggesting hexameric structure.

was applied to the pipette with a screw-driven syringe and monitored with a PM015D (WPI, Sarasota, FL) digital pressure gauge.

For patch imaging, a 60× oil objective and a differential interference contrast (DIC) attachment for the Nikon Diaphot inverted microscope (Nikon, Tokyo, Japan) were used. Pipettes tips were bent at 10–12° to compensate for the tilt of the headstage, which made the axis of the pipette almost parallel to the focal plane. A Hamamatsu Nuvicon tube camera (Hamamatsu, Bridgewater, NJ) with the contrast adjustment device was attached to the microscope via a 4× magnifying adapter and connected to a monitor and a SVHS tape recorder. The images of patches were acquired continuously throughout each experiment and accompanied with audio narration. Selected frames were converted into TIFF files using an Alphaimager 2000 (Alpha Innotech, San Leandro, CA) imaging system. The images were additionally corrected for best contrast, printed in full-page format, and the curvature was assessed manually by applying precision circle templates to the printouts. The tension in the patch membrane (γ) was calculated from the radius of curvature (r) and applied pressure gradient (P) according to the law of Laplace, $\gamma = Pr/2$.

The open probability (Po) at any moment was determined as the number of open channels over the total number of potentially active channels in the patch determined at saturating pressure. The Po pressure curves were converted into $Po(\gamma)$ curves and treated according to the two-state model (Hamill and McBride, 1994; Sukharev et al., 1999a) with the assumption that the occupancies of the closed and open states obey the Boltzmann distribution:

$$Po/Pc = \exp[-(\Delta G - \gamma \Delta A)/kT]$$

ΔG in this equation is the free energy of channel opening in an unperturbed membrane, $\gamma \Delta A$ is the work produced by the external tension as the channel expands for ΔA during the transition, k is the Boltzmann constant, and T is the absolute temperature.

RESULTS AND DISCUSSION

When eluted from the Ni-NTA column with a linear 10–500 mM gradient of imidazole, the MscS-6His protein spreads across several fractions in the second half of the gradient. MscS-6His complexes are displaced from the column with ~300 mM imidazole, suggesting tight binding to the matrix, likely via multiple 6-His groups. Fractions 5–11 (of 11 total) containing the pure 31-kDa band, running slightly faster than predicted by primary sequence, were pooled together. No copurifying proteins were detected. The protein was concentrated 10 times,

transferred into P buffer, and a small volume was subjected to gel filtration. Fig. 1 *A* represents MscS elution from the Superose 6 size-exclusion column. The protein emerges as a relatively sharp peak in two fractions near the 200-kDa mark on the calibration curve. Note that such a distribution has been obtained when lipids (1:100 lipid/detergent molar ratio) are present in the loading, washing, and elution buffers. When only octylglucoside was present, the protein emerged as an ~30-kDa peak, indicating a break-up of multimeric complexes into individual subunits (Fig. 1 *A*, bottom).

Chemical cross-linking experiments were designed to assess the number of subunits in the functional MscS complex. Fig. 1 *B* shows patterns obtained with five different concentrations of DSS used as a bifunctional agent. Even without the cross-linker, MscS exhibits a small amount of dimers, which could be accounted by a frequently observed nonspecific aggregation of membrane proteins. As the concentration of DSS increases, higher ranks appear in the ladder of products. The gradient gel used in this experiment ensured for a relatively even spacing between the multimeric bands. At 1 mM DSS the ladder saturates at the level corresponding to a product, which is approximately six times heavier than the monomer. This pattern has been independently reproduced three times. The sixth band was always most prominent at high concentrations of DSS. It invariably had a fuzzy appearance on gels, suggesting a mixture of cross-linking products in many conformations. Association of six subunits would result in a complex of 186 kDa. The particle size estimated using the gel-filtration chromatography was close to 200 kDa according to calibration using globular standards. This is in reasonable agreement with a hexameric assembly of MscS functional complexes, taking into account the contributions of the detergent and lipids to the size of the complex. The precision of each of the two techniques, however, may be insufficient to make an unequivocal statement about the stoichiometry of MscS. Gel filtration of hydrophobic proteins is inherently ambiguous because of the unknown amounts of lipid and detergent bound to the complex or because of unaccounted interactions with the matrix. Note, that the C-terminal half of MscS is rather hydrophilic, and this increases the chance that the protein behaves in the column more like a soluble one. Covalent cross-linking may also lead to misinterpretations, but the patterns of MscS cross-linking exhibited a clear saturation without extra bands that could suggest otherwise. The pitfalls of these approaches have been discussed previously (Sukharev et al., 1999b), and every result must be taken with caution. With regard to MscS, the two techniques gave coherent results, and the number of subunits forming the complex may be reasonably estimated as six.

Reconstitution of purified MscS-6His in asolectin liposomes at ~1:200 (w/w) protein-to-lipid ratio yielded multiple channel activities in each patch. With relatively large pipettes (2–2.5 μm tip diameter), 7 to 40 channels were routinely observed on first application of pressure and the activities typically saturated between −30 and −60 mm Hg. Subsequent applications of pressure steps or ramps usually yielded less open channels than the first stimulus, indicative of use-dependent channel inactivation. Two representative traces measured with the ascending and the descending series of pressure steps are depicted in Fig. 2. The upper trace shows that MscS first activates at −38 mm Hg, but it takes at least 12 s before the activity reaches a constant level in which 10 channels stay open. A subsequent increase in pressure to −42 mm Hg leads to a further gradual increase in the number of open channels. In ~10 s the current reaches the maximum, and further pressure buildup does not result in any additional increase of the number of open channels (n), which in this particular experiment saturated at $n = 19$. Note that the steep decrease of pressure from −56 to −18 mm Hg results in the closure of most of the channels with a time course that follows approximately the pressure decrease. The observed delayed activation of MscS channels on stepping the pressure up and much faster closure on a pressure release suggested that a descending series of pressures could be a more suitable way of measuring dose-response curves. In the experiment shown in Fig. 2 *B*, the pressure was abruptly stepped up to −30 mm Hg and then released in a stepwise manner. The initial amount of pressure was apparently saturating as it opened all 42 active channels present in the patch and it had to be lowered to −21 mm before a decrease in patch current was observed. The current stabilized within 5–7 s upon each descending step, and the pressure was held for another 5–7 s to confirm that the current level was indeed steady. Longer recordings proved to be unnecessary, as they increased the risk of patch rupture or spontaneous channel inactivation. The arrows above the current trace indicate time points where the readings of the current were deemed stable and could be converted to *Po* values by calculating the ratio of the number of open channels to the total number of initially active channels in the patch. Qualitative observations indicate that reconstituted MscS-6His exhibits a less pronounced time-dependent inactivation and slower transitions as compared with those in spheroplasts reported previously (Koprowski and Kubalski, 1998; Levina et al., 1999). Maintaining constant pressure on a patch for tens of seconds typically elicited almost constant current with infrequent gating events around the mean level.

In an attempt to determine the tension acting on the channel, several large patches were visualized under DIC optics with simultaneous recording of pressure and patch current. In a typical configuration suitable for curvature determination, the patch had to be drawn 20–60 μm deep into the pipette where the bore becomes 5–10 μm wide (Fig. 3). In many instances the second use of the same pipette led to a bigger patch with a more suitable geometry. Complete activation curves in both directions on three independent

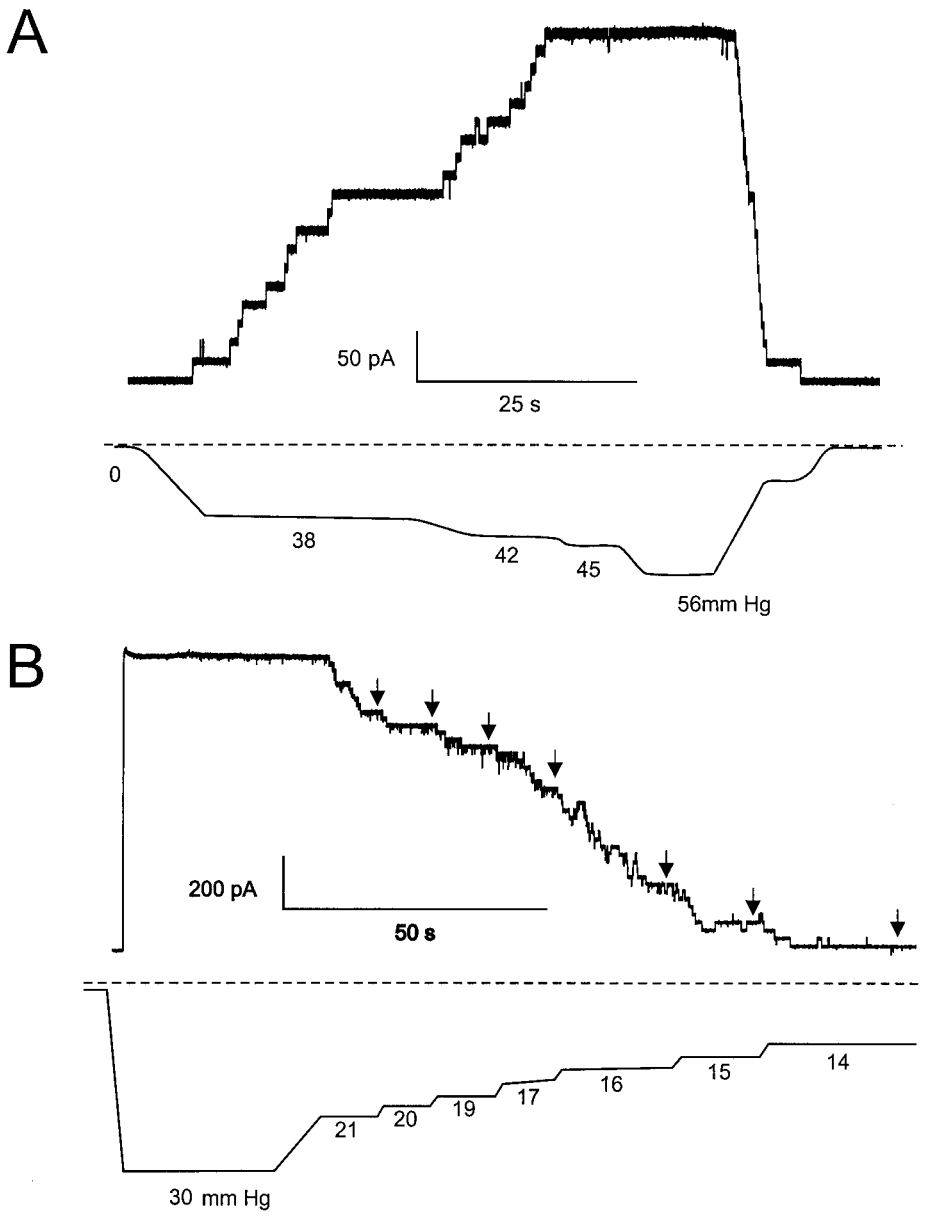

FIGURE 2 Activities of liposome-reconstituted MscS-6His. (*A*) Slow activation of MscS-6His in response to increasing steps of suction (negative pressure) in the pipette. (*B*) Channel activity in response to a saturating pressure gradient, which was then released in a stepwise manner. The *arrows* above the trace indicate the moments at which the channel population comes to equilibrium, which occurs faster in the latter protocol using descending series of pressure gradients. Pressure traces are reproduced schematically.

patches were successfully obtained with images of sufficient quality. Despite the fact that the radii of curvature for the patches varied from 4.1 to 6.7 μm, the resultant $Po(\gamma)$ curves reasonably superimpose (Fig. 4 *A*). The points that correspond to ascending and descending series of pressures are shown with open and filled symbols, respectively. Each group was fit with a sigmoidal Boltzmann-type function. It is evident that the system exhibits a hysteresis as the curves representing the ascending and descending pressure series have the midpoints of 5.9 and 5.5 dyne/cm, respectively, the former being slightly steeper. The simplest explanation for the hysteresis is that because of the delayed activation of MscS, the curves measured with the ascending series do not represent a complete equilibrium at every point. Note that the midpoint of 5.5 dynes/cm is in a reasonable agreement with the previous data by Cui and Adler (1996). The partial activation curves obtained by whole-cell recordings in giant *E. coli* protoplasts shown in Fig. 5 *A* of Cui and Adler (1996) imply a midpoint between 5 and 6 dyne/cm.

To accurately assess the maximal slope of activation curves, *Po* data were collected as a function of pipette pressure for 10 more patches without imaging. Then, assuming that the curves must have the same tension midpoint as for the imaged patches above, $Po(p)$ dependences obtained with descending series of pressures only were transformed into $Po(\gamma)$ curves with $\gamma_{1/2} = 5.5$ dyne/cm. As seen from Fig. 4 *B*, the slopes of individual curves are consistent. The entire dataset was fitted according to the two-state model (Hamill and McBride, 1994; Sukharev et al., 1999a), and the gating parameters were determined. The free energy

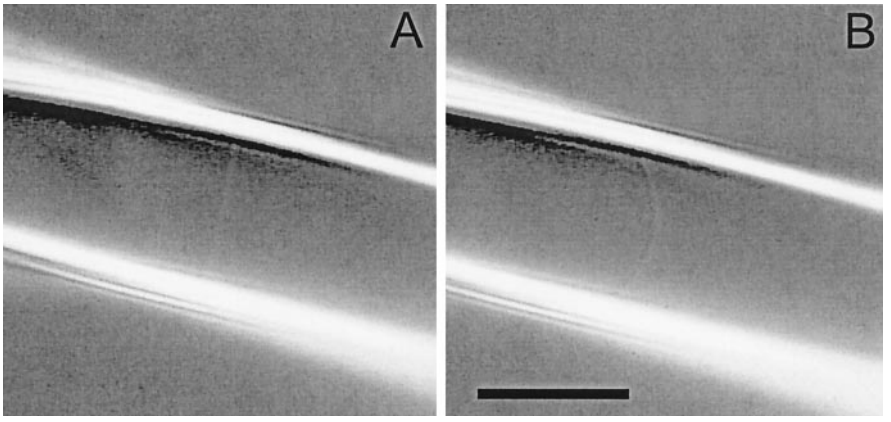

FIGURE 3 Images of a patch taken at the zero pressure (*A*) and at −13 mm Hg (*B*). With the radius of curvature of 6.7 μm, this pressure gradient translates into the tension of 5.8 dyne/cm. Scale bar = 10 μm

of MscS opening, ΔG, was 11.4 kT (or 28.4 kJ/mole) and the in-plane protein expansion, ΔA, was 8.4 nm^2.

The purified and reconstituted MscS-6His channel shows the same asymmetrical current-to-voltage relationship and a slight anionic preference as was previously observed in giant spheroplasts (Martinac et al., 1987) and in reconstituted whole-membrane preparations (Sukharev et al., 1993). Fig. 5 *A* represents I-V curves recorded under symmetrical buffer conditions, (0.1 M KCl bath/0.1 M KCl pipette) and on the same patch after bath perfusion with the buffer containing 0.3 M KCl (○). From the recordings under symmetrical conditions it is evident that slopes of the lines, representing linear regressions for the data at positive and negative pipette voltages, are different (0.54 ± 0.03 nS and 0.27 ± 0.02 nS, respectively). This was reproducibly observed in every patch, suggesting nonrandom orientation of channels in the liposome membrane. The leftward shift of I-V curve observed upon bath perfusion with 0.3 M KCl moved the zero current potential by ~5 mV toward the theoretical reversal potential for Cl^- (−28 mV for a threefold gradient of the ion concentration). Calculations of the relative permeabilities for anions and cations according to the Nernst-Planck or Goldman equations (Zambrowicz and Colombini, 1993) gave similar P_{Cl}/P_K ratios of 1.42 or 1.47, respectively. Thus, reconstituted MscS passes approximately 3 chloride ions per 2 potassium ions.

In addition to the weak anionic selectivity, the channel is characterized with a nonsaturable conductance. Fig. 5 shows that the single-channel conductance is a linear function of the specific bulk conductivity of the buffer up to 1.5 M of salt concentration. This property can be expected for a wide aqueous pore in which ions behave essentially the same way as in the bulk electrolyte. If the pore was totally nonselective, Hille's equation (Hille, 1992) would predict a water-filled cylinder with the radius between 0.7 and 0.9 nm, assuming that the length of the cylinder can be between 3 and 5 nm. However, selectivity implies an electrostatic bias toward a higher concentration of anions at some location in the conducting pathway. The presence of fixed charges inside or near the pore is known to increase the effective electrolyte concentration, making the pore more conductive (Song et al., 1999). Thus, the pore radius of 0.7–0.9 nm (or cross section area of 1.5–2.5 nm^2, respectively) would represent the upper limit for this type of estimation. The observed asymmetry of the I-V curve is consistent with the presence of positive charges near the cytoplasmic entrance. The larger conductance at positive pipette voltages implies a higher concentration of chloride, the more permeant ion, near the inner mouth of the channel. These properties of MscS mirror the behavior of the meningococcal porin A/C1, which is cation-selective and has a large number of negative charges at the extracellular entrance (Song et al., 1999).

The primary sequence of MscS indeed predicts a cluster of positively charged residues (R46, R54, R59, and K50), immediately after the first putative transmembrane domain (Levina et al., 1999). The most recent assessment of MscS topology using the PhoA fusion approach (S. Miller and I.R. Booth, personal communication) suggests that the polypeptide crosses the membrane three times with the N-terminus in the periplasm and the C-terminus inside the cell. This predicts the intracellular location of the positively charged cluster, in agreement with the asymmetrical current-to-voltage relationship. The assumptions on the nature of MscS selectivity, asymmetrical conductance, and pore dimensions, however, require further experimental and theoretical support.

CONCLUSION

Purification of MscS with a polyhistidine tag in the presence of octylglucoside and lipids yields functional complexes of presumably hexameric architecture. MscS-6His reconstituted in liposomes retains most of the functional properties observed in spheroplast patches including mechanosensitivity, indicating that the channel is properly gated by tension in the lipid bilayer. Reconstituted channels, however, show little time-dependent inactivation, which may suggest involvement of other cellular components in this type of

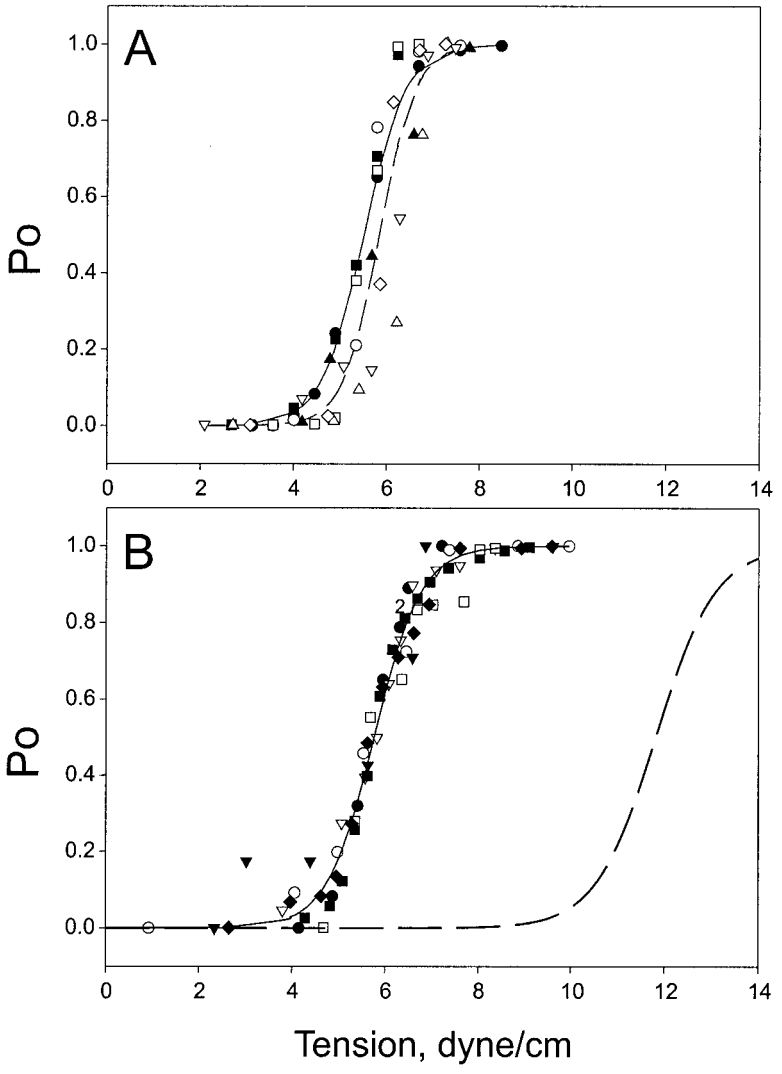

FIGURE 4 Dose-response (open probability vs. tension) curves for liposome-reconstituted MscS-6His. (*A*) Activation curves measured with simultaneous imaging of large liposome patches. Curves from five independent patches measured with ascending series of pressures (○, □, △) exhibit a midpoint of 5.90 ± 0.12 dyne/cm (*dashed line* indicates a sigmoidal curve fit). Three of these patches survived descending series of pressures (●, ■, ▲), showing less data scatter and the midpoint of 5.51 ± 0.07 dyne/cm as determined from the fit (*solid line*). (*B*) A statistical verification of the slope for the MscS-6His dose-response curve. Pressure-activation curves were measured for 10 independent patches without imaging using descending series of pressures and converted into $Po(\gamma)$ curves with the same midpoint of $\gamma_{0.5} = 5.51$ dyne/cm. All data points were fit together according to the equation $Po = 1/1+ \exp[(\Delta G - \gamma\Delta A)/kT]$ (*solid line*), which gave the estimates to the energy for the transition $\Delta G = 11.4 \pm 0.5\ kT$ and the in-plane protein expansion $\Delta A = 8.4 \pm 0.4\ nm^2$. A *dashed line* represents the average position of the MscL activation curve measured in asolectin liposomes (Sukharev et al., 1999).

behavior in the native setting. The liposome-based system permitted determination of the patch curvature and measurement of channel activity as a function of membrane tension. The midpoint of MscS activation (5.5 dyne/cm) is two times lower than that of asolectin-reconstituted MscL (11.8 dyne/cm) (Sukharev et al., 1999a), suggesting that the two types of channels together would provide for a graded response to varied osmotic shocks by activating in a sequential manner. The extracted spatial parameters suggest that opening of MscS pore, which is probably $<2\ nm^2$ in cross section, is accompanied with a larger ($\sim 8.4\ nm^2$) effective in-plane expansion of the channel complex. The conduction asymmetry and ion selectivity correspond well with those recorded in situ, implying that the normal orientation of the channel is retained. The character of single-channel I-V curves was reproducible in many patches, suggesting that the sidedness of channel incorporation into the liposome membrane is not random and may be strongly influenced by the curvature of the bilayer during the removal of the detergent. The question of whether such curvature sensitivity of insertion simply reflects the shape of the protein complex or is critical for the MS channel function needs to be addressed.

MscS has homologs in different bacterial taxons, as well as in archaea, fission yeast, and plants (Levina et al., 1999; Kloda and Martinac, 2001; Koprowski and Kubalski, 2001). It clearly represents a novel channel design. The ability to reconstitute MscS now permits permeability/osmotic shock studies in liposomes as well as complete control over the lipid environment in patch-clamp experiments. This adds one more dimension to the studies of this unusual molecule.

The author thanks Mr. Paul Gray for technical assistance with PCR and Ian Booth (Aberdeen) for strains and critical discussion of the manuscript. Supported by NASA (NAG2–1352) and National Institutes of Health (NS39314–01) research grants.

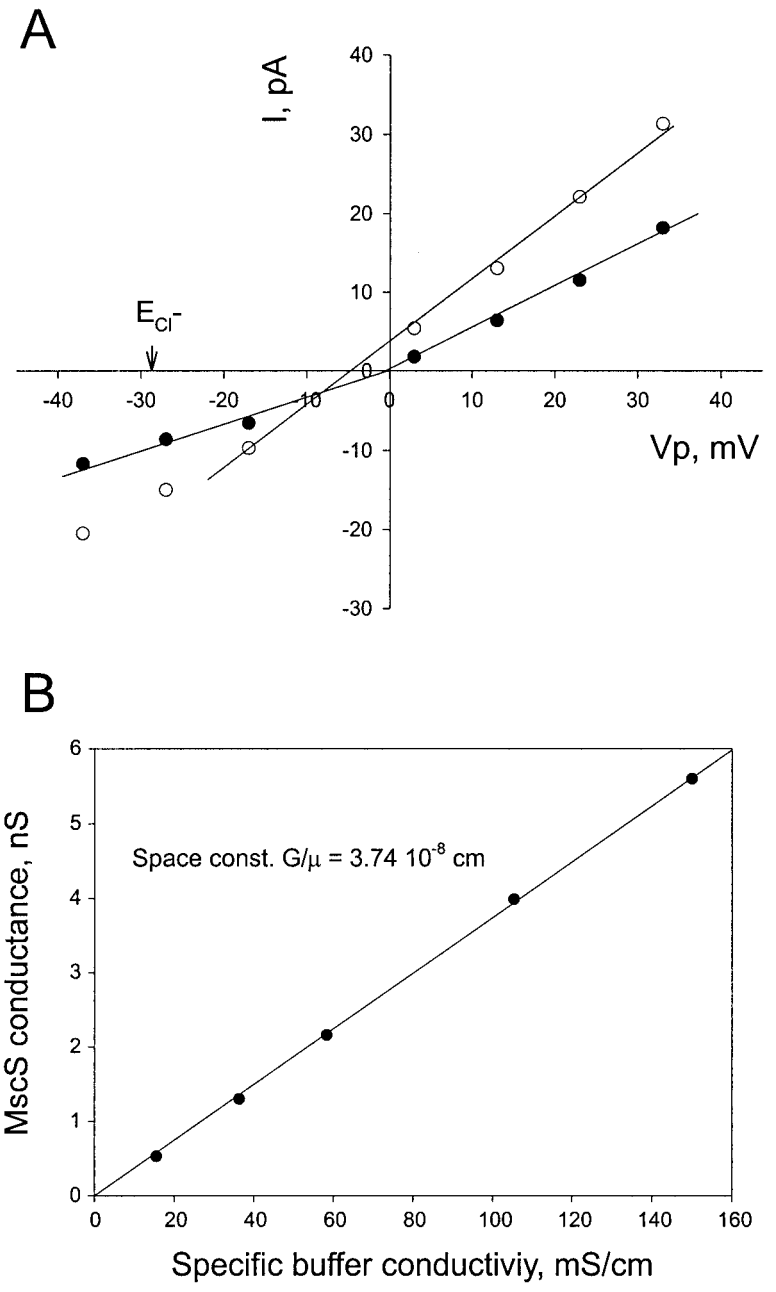

FIGURE 5 Conducting properties of reconstituted MscS-6His. (*A*) Current-to-voltage relationships of the single channel under symmetrical (0.1/0.1 M KCl, ●) and asymmetrical (0.1/0.3 M KCl, ○) ionic conditions. *Straight lines* represent linear regressions. The shift of the zero-current potential toward the reversal potential for Cl^- indicates a slight anionic preference of the channel. (*B*) The single-channel conductance as a function of specific buffer conductivity measured in symmetrical 5 mM HEPES-KOH (pH 7.2) buffers containing 0.1, 0.3, 0.5, 1.0, or 1.5 M KCl.

REFERENCES

Berrier, C., M. Besnard, B. Ajouz, A. Coulombe, and A. Ghazi. 1996. Multiple mechanosensitive ion channels from *Escherichia coli*, activated at different thresholds of applied pressure. *J. Membr. Biol.* 151:175–187.

Blount, P., S. I. Sukharev, P. C. Moe, B. Martinac, and C. Kung. 1999. Mechanosensitive channels of bacteria. *Methods Enzymol.* 294: 458–482.

Blount, P., S. I. Sukharev, P. C. Moe, M. J. Schroeder, H. R. Guy, and C. Kung. 1996. Membrane topology and multimeric structure of a mechanosensitive channel protein of *Escherichia coli*. *EMBO J.* 15: 4798–4805.

Booth, I. R. and P. Louis. 1999. Managing hypoosmotic stress: aquaporins and mechanosensitive channels in *Escherichia coli*. *Curr. Opin. Microbiol.* 2:166–169.

Chang, G., R. H. Spencer, A. T. Lee, M. T. Barclay, and D. C. Rees. 1998. Structure of the MscL homolog from *Mycobacterium tuberculosis*: a gated mechanosensitive ion channel. *Science.* 282:2220–2226.

Chen, R., E. Rosen, and P. H. Masson. 1999. Gravitropism in higher plants. *Plant Physiol.* 120:343–350.

Csonka, L. N. and A. D. Hanson. 1991. Prokaryotic osmoregulation: genetics and physiology. *Annu. Rev. Microbiol.* 45:569–606.

Cui, C., and J. Adler. 1996. Effect of mutation of potassium-efflux system, KefA, on mechanosensitive channels in the cytoplasmic membrane of *Escherichia coli*. *J. Membr. Biol.* 150:143–152.

Delcour, A. H., B. Martinac, J. Adler, and C. Kung. 1989. Modified reconstitution method used in patch-clamp studies of *Escherichia coli* ion channels. *Biophys. J.* 56:631–636.

Gillespie, P. G., and R. G. Walker. 2001. Molecular basis of mechanosensory transduction. *Nature.* 413:194–202.

Hamill, O. P., and D. W. McBride, Jr. 1994. The cloning of a mechanogated membrane ion channel. *Trends Neurosci.* 17:439–443.

Hille, B. 1992. Ionic Channels of Excitable Membranes. Sinauer Asssociates Inc., Sunderland, MA.

Kloda, A., and B. Martinac. 2001. Molecular identification of a mechanosensitive channel in archaea. *Biophys. J.* 80:229–240.

Koch, A. L. 1997. Microbial physiology and ecology of slow growth. *Microbiol. Mol. Biol. Rev.* 61:305–318.

Koprowski, P., and A. Kubalski. 1998. Voltage-independent adaptation of mechanosensitive channels in *Escherichia coli* protoplasts. *J. Membr. Biol.* 164:253–262.

Koprowski, P., and A. Kubalski. 2001. Bacterial ion channels and their eukaryotic homologues. *Bioessays.* 23:1148–1158.

Levina, N., S. Totemeyer, N. R. Stokes, P. Louis, M. A. Jones, and I. R. Booth. 1999. Protection of *Escherichia coli* cells against extreme turgor by activation of MscS and MscL mechanosensitive channels: identification of genes required for MscS activity. *EMBO J.* 18:1730–1737.

Martinac, B., M. Buechner, A. H. Delcour, J. Adler, and C. Kung. 1987. Pressure-sensitive ion channel in *Escherichia coli*. *Proc. Natl. Acad. Sci. U.S.A.* 84:2297–2301.

McLaggan, D., M. A. Jones, G. Gouesbet, N. Levina, S. Lindey, W. Epstein, and I. R. Booth. 2002. Analysis of the *kefA* mutation suggests that KefA is a cation-specific channel involved in osmotic adaptation in *Escherichia coli*. *Mol. Microbiol.* 43:521–536.

Song, J., C. A. Minetti, M. S. Blake, and M. Colombini. 1999. Meningococcal PorA/C1, a channel that combines high conductance and high selectivity. *Biophys. J.* 76:804–813.

Spencer, R. H., G. Chang, and D. C. Rees. 1999. "Feeling the pressure": structural insights into a gated mechanosensitive channel. *Curr. Opin. Struct. Biol.* 9:448–454.

Sukharev, S. I., P. Blount, B. Martinac, F. R. Blattner, and C. Kung. 1994. A large-conductance mechanosensitive channel in *E. coli* encoded by mscL alone. *Nature.* 368:265–268.

Sukharev, S. I., B. Martinac, V. Y. Arshavsky, and C. Kung. 1993. Two types of mechanosensitive channels in the *Escherichia coli* cell envelope: solubilization and functional reconstitution. *Biophys. J.* 65: 177–183.

Sukharev, S. I., M. J. Schroeder, and D. R. McCaslin. 1999b. Stoichiometry of the large conductance bacterial mechanosensitive channel of *E. coli*: a biochemical study. *J. Membr. Biol.* 171:183–193.

Sukharev, S. I., W. J. Sigurdson, C. Kung, and F. Sachs. 1999a. Energetic and spatial parameters for gating of the bacterial large conductance mechanosensitive channel, MscL. *J. Gen. Physiol.* 113:525–540.

Wood, J. M. 1999. Osmosensing by bacteria: signals and membrane-based sensors. *Microbiol. Mol. Biol. Rev.* 63:230–262.

Zambrowicz, E. B., and M. Colombini. 1993. Zero-current potentials in a large membrane channel: a simple theory accounts for complex behavior. *Biophys. J.* 65:1093–1100.